WWW.IJRPR.COM

International Journal of Research Publication and Reviews

Journal homepage: www.ijrpr.com ISSN 2582-7421

Geochemical Characteristics of Neogene Shales form Zakiganj-1 Well at Eastern Folded Flank, Bangladesh: Implication to Delineate the Geochemical Classification, Provenance, Weathering, Climate, Maturity and Tectonic Setting

M. Sahiduzzaman [a,b,*], Moksatara [c], A.S.M. Mehedi Hasan [a,b], Q.H. Mazumdar [b]

[a] *Department of Geology and Mining, University of Rajshahi, Rajshahi-6205, Bangladesh*
[b] *Bangladesh Petroleum Institute (BPI), Uttara Model Town, Dhaka-1230, Bangladesh*
[c] *Department of Disaster Management, Begum Rokeya University, Rangpur-5400.*
DOI: https://doi.org/10.55248/gengpi.5.0224.0527

A B S T R A C T

The Geochemical Classification, Provenance, Weathering, Climate, Maturity and Tectonic Setting of Neogene shales of the Surma Group were delineated from the geochemical analysis of 10 samples collected from Zakiganj Exploration Well-1 at Sylhet Trough. The shales have nearly similar concentration to the average concentration of the upper continental crust, the post-Archean Australian shale. The positive correlations of Al2O3 with other elements as well as the abundance of Ba, Ce, Th, Rb, Zn and Zr suggest that these elements are mainly controlled by the dominant clay minerals. The variations in the geochemistry of their major and trace elements reflect the unstable source conditions and tectonic setting. Tectonic distinction diagrams showed that the shales were largely derived from quartz-rich sediments (quartoze sedimentary provenance), suggesting that they originated from a cratonic interior or recycled orogeny. The binary plots of TiO2 vs. Ni, TiO2 vs. Zr and La/Th vs. Hf, as well as the ternary plots of V-Ni-Th*10 show that the shales and sandstones are derived from felsic igneous rocks. The A-CN-K (Al2O3 -CaO-K2O) ternary diagram and weathering indices (CIA, CIW and PIA) indicate that the granitic source rocks have undergone moderate to high levels of chemical weathering. The lower ratios of V/(V+Ni) and Ni/Co indicate the moderate abundance in the redox state of the oxic depositional environment. The ICV values indicate a medium to high level of maturity. The CIA and ICV presentation show that most shales are geochemically mature and come from both weakly and intensely weathered source rocks. The tectonic position distinction diagrams support both active and passive positions on the continental margin of origin.

Keywords: Geochemistry, Provenance, Tectonic settings, Zakiganj-1 well, Neogene Shale, Surma Basin

1. Introduction

The geochemistry is important for understanding the evolution of provenance and source weathering and the source nature of clastic sedimentary rocks is well established [1], [2], [3], [4], [5], [6]. The chemical and mineralogical composition can be influenced to some extent by factors such as source rock properties, weathering, sorting processes during transport, sedimentation and diagenetic processes [7]. Trace elements such as La, Y, Sc, Cr, Th, Zr, Hf, Nb and rare earth elements (REE) are considered useful indicators of origin, geological processes and tectonic processes due to their relatively low mobility and insolubility during sedimentation [8]. Therefore, the geochemistry of clastic sediments (i.e., shale) reflects a combination of provenance, chemical weathering, hydraulic sorting, and abrasion [5], [6], [9], [10].

The fine-grained sedimentary rocks such as shales are considered as the most useful rock in geochemical provenance studies due to their homogeneity before deposition, their impermeability after deposition, and their higher abundance of trace elements [7], [11], [12], [13]. Some relatively immobile elements such as Sc, Th, Zr, Hf and rare earth elements (REE) have very low concentrations in natural waters and are almost quantitatively transported from the parent rock to the clastic sediments during the sedimentation process [9], [14]. The relative distribution or enrichment of these immobile elements in felsic and basic rocks has been used to infer the relative contribution of felsic and basic sources in shales from different tectonic environments [15].

Several authors studied on Neogene shales of Surma Group, among them Rahman and Faupl [16] analysed Neogene shale from Atgram-1, Beanibazar-1, Fenchuganj-2, Patharia-5 and Rashidpur-3 wells. Thereafter, Rahman and Faupl [16] and Rahman and Suzuki [17] analyzed Neogene shale from Shahbazpur-1, Shaldanadi-1 and Titas-11 exploratory wells. However, there is no any previous geochemical study of Neogene shale from Zakiganj-1 exploratory well. As the Zakiganj-1 exploratory well shows petroleum reserve, further research may be needed for petroleum production. The detail study on geochemical characteristics of Neogene shale Zakiganj-1 exploratory well will provide the important information for further research. So, it is necessary to explore the geochemical classification, provenance, weathering, climate, maturity and tectonic setting of Neogene shale of the Zakiganj-1 well. It could be a ready attribution for any further Exploratory/ Production wells in Zakiganj field.

2. Geological Setting

The Bengal Basin is bounded on the north by the Shillong Massif, east and south-east by the Chittagong- Tripura fold belt of the Indo-Burman ranges and west by the Indian Shield Platform. The fold belt is characterized by series of meridional to sub-meridional folds and extends into the Indian territory of Tripura and Mizoram to the east. Also known as frontal fold belt, this province represents the western and outermost part of the Indo-Burman origin. The fold belt shows sign of diminishing intensity of structures towards the west in which direction it gradually fades away and merge with the central foredeep province [18]. Zakiganj is the extreme northern edge of the Patharia Hill structure which belongs to the Sylhet Trough (figure 1).

The Sylhet Trough is a sub-basin of the Bengal Basin in the northeastern part of Bangladesh. It was structurally developed by the simultaneous interaction of two major tectonic movements: (1) the northward uplift of the Shillong Massif and (2) the westward spreading of the mobile Indo-Burman fold belt [19]. Johnson and Alam [20] proposed that the Sylhet Trough developed from a passive pre-Oligocene continental margin to a foreland basin associated with the Indo-Burman Ranges during the Oligocene and Miocene. Since the Pleistocene, this basin has been associated with the south-facing thrust of the Shillong Plateau. The Sylhet Trough formed part of the foreland basin of the Himalayan orogeny and the Indo-Burman Mountains (active continental margin). Subsidence began at least from the Oligocene onwards [21]. The depression is bounded to the east and southeast by the Chittagong-Tripura fold belt (CTFB) of the Indo-Burman Ranges and to the west by the Indian Shield platform. To the north, the Shillong shield plateau borders the hollow. The Dauki fault system with large vertical displacements represents the contact between the Sylhet Trough and the Shillong Plateau [19], [20]. The trough is open to the south and southeast towards the main part of the Bengal Basin.

The Sylhet Trough contains a 12 to 16 km thick fill of late Mesozoic and Cenozoic strata [20]. Lithologically, the Surma Group consists of a succession of alternating shales, silts, sandstones (figure 2) and sandstones with occasional conglomerate layers [21]. Johnson and Alam [20] suggested that the Miocene strata of the Surma Group were predominantly deposited in a large, mud-rich delta system that drained a large portion of the eastern Himalayas. The Suma Group is overlain by Tipam Group and underlain by Barail Group [22], [23]. The Tipam group comprises the Tipam Sandstone Formation and Girujan Clay Formation. The Barail Group comprises the Laisong Formation, Jenam Formation and Renji Formation. The stratigraphic succession of the Sylhet Trough [22] (Pliocene* magnetostratigraphic age after Worm [23]) is shown in Table 1.

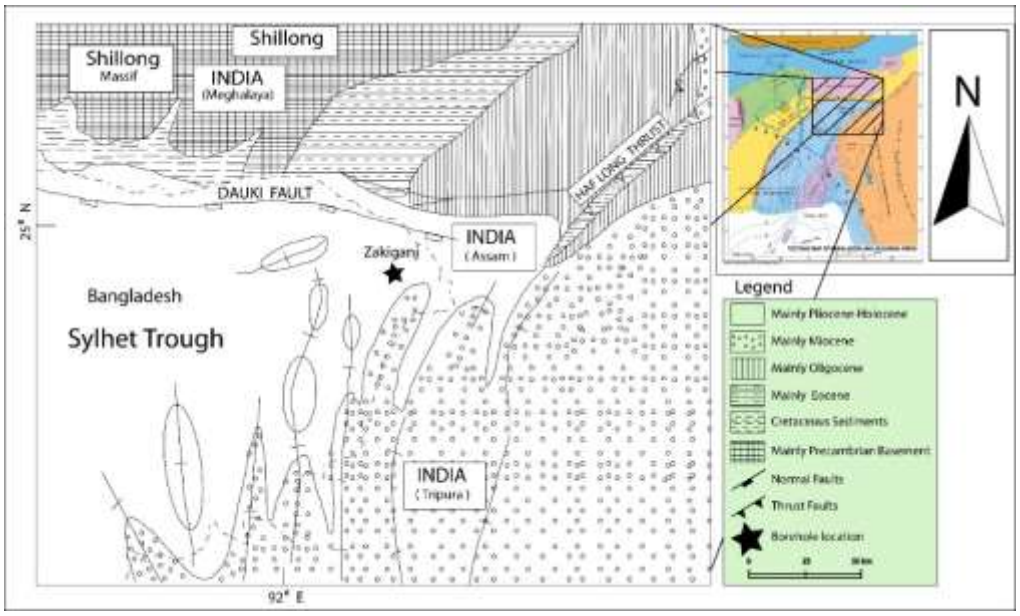

Fig. 1 - Location Map of the Zakiganj - 1 Well (modified after Rahman et.al., 2003).

Table 1 - The stratigraphic succession of the Zakignaj- 1 well [22] (modified after Zakiganj – 1 well completion report of BAPEX, 2021).

Age (approx..)	Group	Formation	Lithology	Depositional Environment	Depth (m)
Pliocene	Tipam Group	Girujan Clay Formation	Clay, Sandstone	Fluvial lacustrine	0 to 240
		Tipam Sandstone Formation	Predominantly sandstone with minor shale and clay beds	Fluvial	240 to 1,220
	Surma Group	Boka Bil Formation	Alternating shale and sandstone with minor siltstone		1,220 to 2,865
Pliocene Miocene	Study Section	Bhuban Formation	Alternating and repetitive sandstone and shale with minor siltstone	Marine deltaic	2,865 to not determined (Total drilling depth 2,980 m)

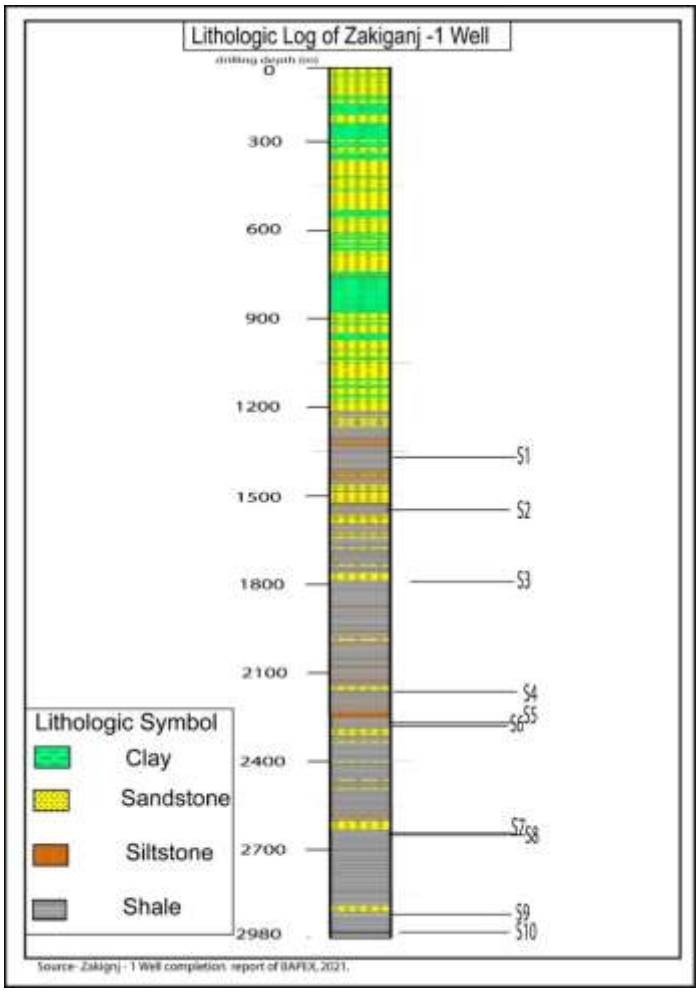

Fig. 2 - Lithologic log of Zakiganj-1 well (modified after Zakiganj - 1 completion report of BAPEX, 2021).

3. Materials and Methods

Zakiganj Well-1 was drilled in 2020-2021 by Bangladesh Petroleum Exploration and Production Company Limited (BAPEX). Geographically, it is located at Madhu Datta Mouza of Zakiganj Pourashava under Zakiganj Upazila in Sylhet district. The target depth was 3100 m (±100 m), but was drilled upto a depth of 1,981 m. Ten samples with various depth of Neogene shale representing Zakiganj Well-1 were collected from Longitude: 92º2'45.00"E and Latitude: 24º59'0.924"N. All the analyses and discussions were accomplished based on these 10 samples.

3.1 X-ray Fluorescence (XRF)

The samples were analyzed for concentrations of major and trace elements (including rare earth elements). X-ray fluorescence (XRF) analysis was performed at Activation Laboratories Ltd., 41 Bittern Street, Ancaster, Ontario, L9G 4V5 Canada (Report Number: A23-07505, Report Date: 12/6/2023). The major elements were analyzed using Fusion Inductively Coupled Plasma (FUS-ICP), in which an oxidized sample were dissolved in a borate flux and then diluted in aqueous nitric acid. Inductively Coupled Plasma Optical Emission Spectroscopy (ICP-OES) was used to quantify various elements in the resulting solution. The concentrations of trace elements and rare earth elements were determined by FUS-MS (Fusion-inductively Coupled Plasma Mass Spectrometry), in which an oxidized sample was dissolved in a borate flux and then diluted in aqueous nitric acid. ICP-MS (Inductively Coupled Plasma Mass Spectrometry) was used to quantify various elements in the resulting solution.

3.2 Analytical Tools

The MS Excel and SPSS (Statistical Package for the Social Sciences) were used for statistical calculations. The Geo-chemical Data ToolKIT (GCDkit) was used for standard geochemical calculations with major and trace elements and for plotting binary, ternary and spider diagrams. The graphic software as adobe illustrator and adobe Photoshop were used for further modification of various figures.

4. Results

The geochemical composition of the representative studied samples presents in Table 2, 3 and 4.

Table-2: The major elements abundances in the investigated Neogene Shale of Zakiganj- 1well.

Analyte Symbol	S-1	S-2	S-3	S-4	S-5	S-6	S-7	S-8	S-9	S-10	Avg	Min	Max
SiO_2	63.25	58.6	55.41	55.5	58.32	53.07	52.98	51.56	54.09	50.85	55.36	50.8	63.25
Al_2O_3	13.5	15.9	15.99	14.76	15.13	14.27	14.54	14.02	16.07	15.31	14.95	13.5	16.07
Fe_2O_3(T)	6.1	6.44	6.16	6.06	6.01	5.93	5.62	5.75	6.52	5.94	6.05	5.62	6.52
MnO	0.103	0.101	0.102	0.111	0.096	0.095	0.099	0.086	0.099	0.091	0.10	0.09	0.11
MgO	2.29	2.48	2.28	2.77	2.75	2.65	2.16	1.93	2.19	1.95	2.35	1.93	2.77
CaO	1.89	1.66	1.23	2.26	2.34	2.1	0.99	0.89	0.74	0.53	1.46	0.53	2.34
Na_2O	1.31	1.22	1.21	1.24	1.33	1.3	1.43	1.36	1.21	1.28	1.29	1.21	1.43
K_2O	3.28	3.87	5.24	4.51	4.25	5.6	4.86	5.02	4.76	5.1	4.65	3.28	5.60
TiO_2	0.772	0.807	0.788	0.714	0.735	0.697	0.648	0.62	0.719	0.623	0.71	0.62	0.81
P_2O_5	0.12	0.15	0.15	0.14	0.15	0.15	0.12	0.12	0.12	0.13	0.14	0.12	0.15
LOI	6.5	8	9.59	8.73	8.04	10.87	10.47	11.73	8.12	9.53	9.16	6.50	11.73
Total	99.12	99.24	98.14	96.8	99.14	96.73	93.92	93.1	94.63	91.35	96.22	91.35	99.24
Na_2O/K_2O	0.399	0.315	0.231	0.275	0.313	0.232	0.294	0.271	0.254	0.251	0.28	0.23	0.40
Fe_2O_3 + MgO	8.39	8.92	8.44	8.83	8.76	8.58	7.78	7.68	8.71	7.89	8.40	7.68	8.92
Al_2O_3/TiO_2	17.487	19.703	20.292	20.672	20.585	20.473	22.438	22.613	22.350	24.575	21.12	17.49	24.57
log (Na_2O/K_2O)	-0.40	-0.50	-0.64	-0.56	-0.50	-0.63	-0.53	-0.57	-0.59	-0.60	-0.55	-0.64	-0.40
log (SiO_2/Al_2O_3)	0.67	0.57	0.54	0.58	0.59	0.57	0.56	0.57	0.53	0.52	0.57	0.52	0.67
SiO_2/Al_2O_3	4.69	3.69	3.47	3.76	3.85	3.72	3.64	3.68	3.37	3.32	3.72	3.32	4.69
K_2O/Na_2O	2.50	3.17	4.33	3.64	3.20	4.31	3.40	3.69	3.93	3.98	3.62	2.50	4.33
CIA	68	70	68	65	66	61	67	66	71	69	66.90	61.32	70.54
CIW	81	85	87	81	80	81	86	86	89	89	84.48	80.48	89.43
PIA	76	81	82	75	75	72	80	80	85	85	78.97	71.83	85.29
ICV	0.99	0.88	0.91	1.00	0.97	1.10	0.93	0.97	0.87	0.88	0.95	0.87	1.10
IA	40	41	40	39	40	38	40	40	41	41	40.07	38.01	41.36

Table 3 - The trace elements concentrations in the investigated Neogene Shale of Zakiganj- 1well.

Analyte Symbol	S-1	S-2	S-3	S-4	S-5	S-6	S-7	S-8	S-9	S-10	Avg	Min	Max
Be	3	3	3	3	3	3	2	3	3	3	2.90	2.00	3.00
V	101	117	114	104	105	105	101	100	116	106	106.90	100.00	117.00
Cr	100	130	120	110	110	110	110	110	120	110	113.00	100.00	130.00
Co	17	19	19	18	17	17	17	17	18	17	17.60	17.00	19.00
Ni	50	60	60	50	50	50	60	60	60	60	56.00	50.00	60.00
Cu	20	30	20	20	30	20	40	30	30	30	27.00	20.00	40.00
Zn	70	90	90	80	80	80	80	80	80	90	82.00	70.00	90.00
Ga	21	24	24	22	23	22	22	22	25	23	22.80	21.00	25.00
Ge	1.5	1.5	1.5	1.5	1.5	1.4	1.7	1.4	1.7	1.6	1.53	1.40	1.70
As	7	8	8	6	6	7	10	8	7	7	7.40	6.00	10.00
Rb	130	150	144	148	151	146	141	137	155	149	145.10	130.00	155.00
Sr	131	126	124	114	115	144	190	197	160	193	149.40	114.00	197.00
Zr	237	188	176	172	194	166	147	159	170	146	175.50	146.00	237.00
Nb	12.4	14.6	14.2	12.7	13.4	13	12	11.6	12.8	11.8	12.85	11.60	14.60
Mo	< 2	< 2	< 2	< 2	< 2	< 2	< 2	< 2	< 2	< 2	-	0.00	0.00
Ag	< 0.5	< 0.5	< 0.5	< 0.5	< 0.5	< 0.5	< 0.5	< 0.5	< 0.5	< 0.5	-	0.00	0.00
In	0.1	0.1	0.1	0.1	0.1	0.1	0.1	0.1	0.1	0.1	0.10	0.10	0.10
Sn	3	4	3	3	4	3	4	3	4	4	3.50	3.00	4.00
Sb	0.4	0.4	0.3	0.3	0.3	0.3	0.7	0.4	0.4	0.5	0.40	0.30	0.70
Cs	8.6	10	9.6	8.6	8.8	8.7	9.4	8	9.4	8.9	9.00	8.00	10.00
Ba	4410	8544	15060	11610	8592	34000	55360	68350	36130	71150	31320	4410.00	71150
Hf	6.2	5.3	4.8	4.6	5.3	4.6	4.2	4.6	4.5	4	4.81	4.00	6.20
Ta	1.09	1.08	0.98	0.98	1.05	0.94	0.87	0.88	1.03	0.84	0.97	0.84	1.09
W	11.3	6	3.6	5.5	15.2	8.6	14	4.6	4.7	4.3	7.78	3.60	15.20
Tl	0.5	0.53	0.38	0.41	0.44	0.28	0.37	0.31	0.48	0.35	0.41	0.28	0.53
Pb	18	21	20	19	20	18	34	24	26	28	22.80	18.00	34.00
Bi	< 0.1	0.1	< 0.1	< 0.1	< 0.1	0.1	0.2	< 0.1	< 0.1	0.2	0.15	0.10	0.20
Th	16.5	15.5	15.2	15	15.6	14.7	13.8	13.1	16	12.9	14.83	12.90	16.50
U	2.85	2.65	2.46	2.54	2.81	2.58	2.52	2.59	2.92	2.5	2.64	2.46	2.92

Table 4 - The rare earth elements concentrations in the investigated Neogene Shale of Zakiganj- 1well.

Analyte Symbol	S-1	S-2	S-3	S-4	S-5	S-6	S-7	S-8	S-9	S-10	Avg	Min	Max
Sc	14	15	15	14	14	14	14	14	16	15	14.50	14.00	16.00
Y	30	31.2	29.1	28.5	29.9	28.1	26.9	27.4	29.3	25.7	28.61	25.70	31.20
La	38.2	39.2	38.4	36.4	37.7	36	34.6	34.7	37	32.4	36.46	32.40	39.20
Ce	73.7	75.7	75	70.5	72.3	71	66.4	65.6	71.3	61.6	70.31	61.60	75.70
Pr	9.19	9.48	9.3	8.74	9.01	8.84	8.27	8.2	9	7.85	8.79	7.85	9.48
Nd	33.8	34.3	33.2	31.7	32.3	31.6	29.9	30.5	32.7	27.9	31.79	27.90	34.30
Sm	6.72	6.82	6.8	6.35	6.43	6.37	6.01	6.08	6.65	5.77	6.40	5.77	6.82
Eu	1.22	1.19	1.01	1.01	1.08	0.579	0.192	< 0.005	0.404	< 0.005	0.84	0.19	1.22
Gd	5.96	5.83	5.65	5.23	5.56	5.38	5.13	5.19	5.6	4.82	5.44	4.82	5.96
Tb	0.9	0.86	0.82	0.81	0.86	0.81	0.81	0.74	0.86	0.73	0.82	0.73	0.90
Dy	5.32	5.21	5.12	4.95	5.01	5.07	4.91	5.06	5.49	4.59	5.07	4.59	5.49
Ho	1.06	1.04	1.05	0.93	1	0.94	0.92	0.97	1.04	0.92	0.99	0.92	1.06
Er	3.09	2.95	2.94	2.7	2.86	2.85	2.73	2.79	3.07	2.78	2.88	2.70	3.09
Tm	0.456	0.421	0.416	0.389	0.419	0.413	0.404	0.4	0.456	0.405	0.42	0.39	0.46

Yb	2.75	2.62	2.59	2.46	2.61	2.57	2.5	2.5	2.83	2.53	2.60	2.46	2.83
Lu	0.452	0.44	0.42	0.42	0.43	0.39	0.41	0.42	0.45	0.4	0.42	0.39	0.45

4.2 Major Elements

The major elemental compositions of Zakiganj-1 well have a wide range of variation, namely, SiO_2 (%) from 50.85 to 63.25 with an average of 55.36, Al_2O_3 (%) from 13.50 to 16.07 with an average of 14.95, Fe_2O_3(T) (%) from 5.62 to 6.52 with an average of 6.05, K_2O (%) from 3.28 to 5.60 with an average of 4.65 and so on (Table 2). Stratigraphically, the highly concentrated SiO_2 variations show continuously decreasing trends with increasing depth. The burial depth of the samples is shown in Figure 3. The average major element composition of the samples examined is quite similar to that of the average shale according to Turekan and Wedepohl [24], with the exception of the CaO content. The CaO depletion of the studied samples is concerned to the scarcity of calcareous minerals [25]. The SiO_2 concentration in the studied shale is lower than the average of the upper continental crust (UCC), the post-Archean Australian shale (PASS), and the North American shale composite (NASC) [11], [26], [27], [28] (Table 5). The behavior of most of the major oxides, trace and rare earth elements as TiO_2, MgO, MnO, CaO, P_2O_5 and Fe_2O_3, Be, V, Co, Zr, Nb, Cs, La, Ce, Pr, Nd, Sm show the positive trend with SiO_2 while Al_2O_3, K_2O, Na_2O, Cr, Ni, Cu, Ga, Ge, As, Rb, Sr, Sc, Sn, Sb show negative trend (Table 6). Moderately concentrated Al_2O_3 is more or less similar to average Shale after Pettijohn [29], average Shale after Turekan and Wedepohl [24], UCC, PASS and NASC. Among the major oxides TiO_2, MgO, K_2O, P_2O_5 and trace and rare earth elements as Cr, Ce, Rb, Y, La show the positive correlation trend with Al_2O_3 while CaO and Na_2O of major oxides and Sr, Zr, Ba of trace and rare earth elements show negative concentration trend. The positive correlation trends of these major oxides with Al_2O_3 infers that they are associated with micaceous/clay minerals [30]. The TiO_2 concentrations increase with Al_2O_3, indicating that TiO_2 is likely associated with phyllosilicates, particularly illite [25]. The positive correlations of K_2O, Fe_2O_3, MgO and TiO_2 with Al_2O_3 (table 6), indicates a large influence of hydraulic fractionation [31].

Table 5 - Comparison of the average major oxides of the Neogene Shale of Zakiganj Well- 1 with published average shales.

Oxides	**Shale concentration in this study**	**Average Shale after Pettijohn** [32]	**Average Shale after Turekan & Wedepohl** [24]	**UCC after Rudnick** [27]	**PASS after Taylor, & McLennan**[11]	**NASC after Gromet**[28]
SiO_2 (%)	55.36	59.10	58.50	66.60	62.40	64.82
TiO_2 (%)	0.71	0.60	0.77	0.64	0.99	0.80
Al_2O_3 (%)	14.95	15.40	15.00	15.40	18.78	17.05
Fe_2O_3(T) (%)	6.05	6.90	4.72	5.04	7.18	5.70
MnO (%)	0.10	Trace	-	0.10	0.11	-
MgO (%)	2.35	2.40	2.50	2.48	2.19	2.83
CaO (%)	1.46	3.10	3.10	3.59	1.29	3.51
Na_2O (%)	1.29	1.30	1.30	3.27	1.19	1.13
K_2O (%)	4.65	3.20	3.10	2.80	3.68	3.97
P_2O_5 (%)	0.14	0.20	0.16	0.12	0.16	0.15

The samples were normalized to UCC [27] and PASS [11] as shown in Figure 4. Relative to UCC, the average normalized values relative to UCC of SiO_2, Al_2O_3, Fe_2O_3, MnO, MgO, TiO_2 and P_2O_5 in the Neogene Shale of Zakiganj-1 well are 0.83, 0.97, 1.20, 0.98, 0.95, 1.11 and 1.13 respectively which are easily comparable with the UCC. Al and Ti are readily absorbed by clay and concentrate in the finer, more weathered materials [33]. The average normalized values of K2O relative to UCC is 1.66 which is high as compared to UCC and the average normalized values relative to UCC of CaO and Na_2O are 0.41 and 0.39 which are low as compared to UCC. The depletion of Na_2O (<1%) in the Neogene Shale of Zakiganj-1 Well can be attributed to a relatively smaller amount of Na-rich plagioclase in them. K_2O and Na_2O contents and their ratios (K_2O/NaO>1) showed that K-feldspar dominates over plagioclase-feldspar (albite). The K_2O enrichment is related to the presence of illite as a common clay mineral in shales. In addition, the enrichment of CaO (avg. 0.41 relative to UCC) can be ascribed to the existence of diagenetic calcite cement.

The average normalized values relative to PASS of SiO_2, TiO_2, Al_2O_3, Fe2O_3(T), MnO, MgO, CaO, Na_2O, K_2O and P_2O_5 are 0.89, 0.72, 0.80, 0.84, 0.89, 1.07, 1.13, 1.08, 1.26 and 0.84 respectively which are easily comparable with the PASS.

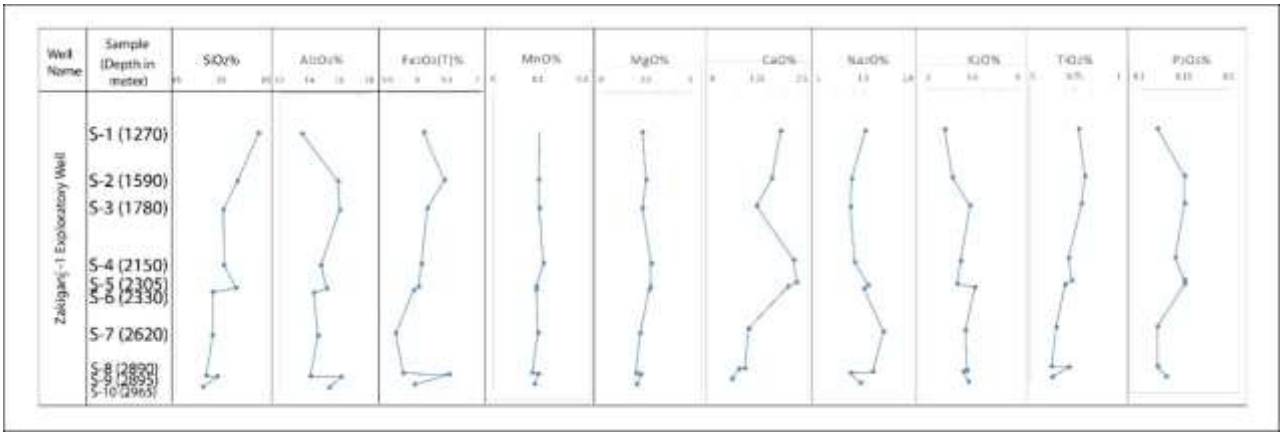

Fig. 3 - Major chemical composition of Neogene Shale of Zakiganj- 1 well in relation to depth of burial.

a

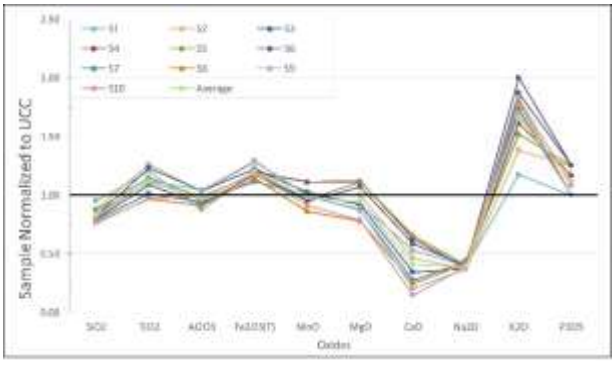

b

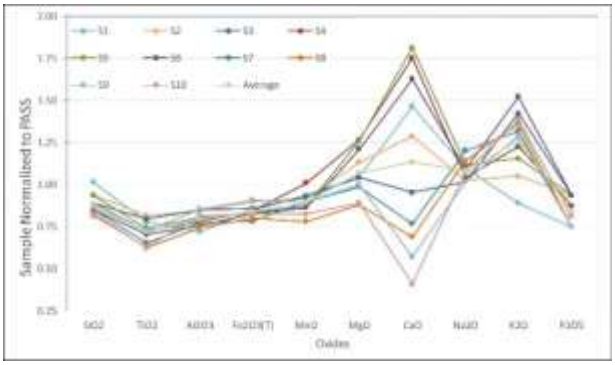

c

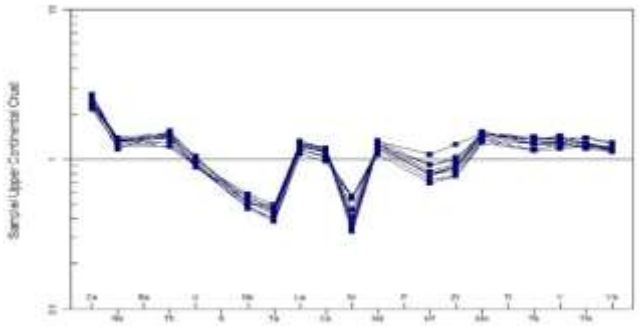

d

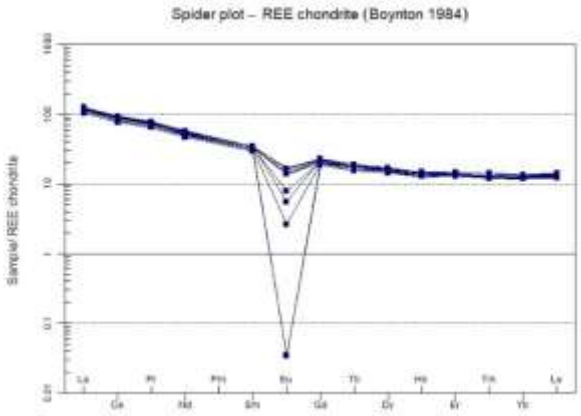

Fig. 4 - Spider plot of major Oxides showing (a) shales normalized against UCC (b) shales normalized against PASS. c) Trace and rare earth elements normalized against UCC [11] **d) Chondrite-normalized REE diagram** [34]**.**

Table 6- Pearson Coefficients of major elements, Trace elements and rare earth elements.

Symbols	**SiO_2**	**Al_2O_3**	**$Fe_2O3(T$**	**MnO**	**MgO**	**CaO**	**Na_2O**	**K_2O**	**TiO_2**	**P_2O_5**	**Sc**	**Be**	**V**	**Cr**	**Co**	**Ni**	**Cu**	**Zn**	**Ga**	**Ge**	**As**	**Rb**	**Sr**	**Y**	**Zr**	**Nb**
SiO2	1																									
Al_2O_3	-0.2	1																								
$Fe_2O_3(T)$	0.4	0.64	1																							
MnO	0.5	0.2	0.4	1																						
MgO	0.4	0.0	0.2	0.6	1																					
CaO	0.6	-0.3	0.1	0.5	.9	1																				
Na_2O	-0.2	-.6	-.8	-0.4	-0.2	-0.1	1																			
K_2O	-.8	0.2	-0.4	-0.4	-0.2	-0.4	0.1	1																		
TiO_2	.7	0.3	.7	0.6	0.5	0.5	-0.6	-0.5	1																	
Sc	-0.2	.8	.7	0.0	-0.3	-0.6	-.6	0.1	0.2	-0.1	1															
Be	0.2	0.2	0.5	0.0	0.2	0.2	-.6	-0.1	0.3	0.4	0.2	1														
V	0.1	.8	.8	0.2	0.1	-0.2	-.8	0.0	0.6	0.4	.8	0.3	1													
Cr	-0.1	.8	.6	0.1	0.0	-0.2	-0.6	0.1	0.4	0.4	.6	0.1	.8	1												
Co	0.2	.7	.6	0.5	0.2	0.0	-.7	-0.1	.6	0.5	0.6	0.3	.8	.8	1											
Ni	-0.5	0.5	0.1	-0.4	-.7	-.8	-0.1	0.3	-0.2	-0.3	0.6	-0.3	0.4	0.6	0.4	1										
Cu	-0.4	0.2	-0.3	-0.4	-0.4	-0.5	0.5	0.0	-0.5	-0.4	0.1	-.6	-0.1	0.2	-0.2	0.6	1									
Zn	-0.4	.7	0.2	-0.1	-0.2	-0.4	-0.4	0.4	0.1	0.5	0.5	0.1	0.6	.7	0.6	0.6	0.2	1								
Ga	-0.2	.9	.713*	0.0	-0.1	-0.4	-.6	0.2	0.3	0.3	.8	0.2	.9	.8	.6	0.6	0.2	0.6	1							
Ge	-0.2	0.4	0.1	0.2	-0.3	-0.5	0.0	0.0	-0.2	-0.5	0.5	-0.6	0.2	0.1	0.0	0.4	0.6	0.1	0.4	1						
As	-0.3	0.0	-0.4	-0.2	-0.5	-0.5	0.5	0.2	-0.2	-0.3	0.0	-.7	0.0	0.2	0.1	.6	0.6	0.2	0.0	0.3	1					
Rb	-0.3	.7	0.5	0.1	0.3	0.0	-0.5	0.3	0.1	0.4	0.6	0.2	.6	0.6	0.4	0.2	0.2	0.5	.7	0.3	-0.3	1				
Sr	-.7	-0.2	-0.5	-.7	-.8	-.8	0.5	0.4	-.8	-.6	0.1	-0.4	-0.3	-0.2	-0.5	0.6	0.6	0.1	-0.1	0.3	0.5	-0.2	1			
Y	.8	0.2	.7	0.5	0.5	0.6	-0.5	-.6	.9	0.4	0.1	0.4	0.5	0.4	0.5	-0.3	-0.3	-0.1	0.3	-0.2	-0.3	0.1	-.7	1		
Zr	0.9	-0.3	0.4	0.4	0.4	0.6	-0.2	-.81	.7	0.1	-0.2	0.4	0.0	-0.2	0.1	-0.5	-0.5	-0.5	-0.2	-0.3	-0.4	-0.4	-.6	.7	1	
Nb	0.4	0.6	0.6	0.4	0.5	0.4	-0.6	-0.2	.8	.7	0.3	0.3	.7	.7	.7	0.0	-0.3	0.4	0.5	-0.2	-0.1	0.4	-.7	.7	0.3	1

4.2 Trace Elements

Various types of trace elements were found in the sediment studied samples of Zakiganj-1 well, for example Large Ion Lithophile Elements (LILE), High Field Strength Elements (HFSE) and Transition Trace Elements (TTE). The Large Ion Lithophile Elements (LILE) are comparatively mobile and incompatible elements. The average concentrations of LILE such as Rb is 145 ppm with minimum 130 ppm and maximum 155 ppm, Sr is 149 ppm minimum 114 ppm and maximum 197 ppm and Cs is 9 ppm with minimum 8 ppm and maximum 10 ppm. The Trace and rear earth elements were normalized against UCC average upper crust composition (UCC) [11] as shown in Figure 4c. The average concentrations of Cs and Rb are higher than the average upper crust composition (UCC) while Sr lower than the average UCC. Cs and Rb show a relatively strong linear positive correlation with Al_2O_3 (table 6) indicating an understandable hydraulic fractionation [31], [35]. Ba and Sr show a moderate positive correlation trend with Al_2O_3. Strong positive correlations of mobile components indicate their relationship to finer particles, indicating the hydraulic distribution of quartz and clay. HFSEs are incompatible but immovable elements which are enriched in felsic rather than mafic rocks [36]. Because of their immobility, The HFSEs are considered as the provenance indicators [11]. The average concentration of Zr is 175.5 ppm with minimum concentration 146 ppm and maximum 237 ppm. The concentration of Y ranges from minimum of 26 ppm to maximum of 31 ppm with an average of 28.61 ppm. The concentration of Nb ranges from minimum of 12 ppm to maximum of 15 ppm with an average of 12.85 ppm. The concentration of Nb is slightly lower than UCC while the concentration of Y and Zr are nearly similar. The transition trace elements (TTE) such as Sc, V, Cr, Ni and Zn range from 14 to 16 ppm with an average 14.50 ppm, 100 to 117 ppm with an average 106.90 ppm, 100 to 130 ppm with an average 113 ppm, 50 to 60 ppm with an average 56 ppm and 70 to 90 ppm with an average 80 ppm, respectively. The Rare earth elements (REE) such as Yb, La, Ce, Sm are similar to UCC. The Hf and Th are slightly depleted to UCC but U is similar.

The rare earth elements (REEs) are a very useful geochemical tool that could provide valuable information about rock formation. The REEs comprise the group of lanthanides, which includes 14 elements from lanthanum (La) to lutetium (Lu). Taylor and Mclennan (1985) assumed that REEs are richer in the upper crust than in the lower crust. The lanthanides are known for their very similar chemical and physical properties. They (as well as U and Th) behave incompatible in magmatic processes. However, crystallization of small amounts of accessory minerals (from larger cation sites) such as zircon, garnet, monazite, allanite, xenotime, apatite, and sphene would control the REEs content during magma crystallization and could lead to depletion of REEs in the residual fluids [37]. Chondrite-normalized REE diagrams [34] of the studied shales show a negative correlation with Eu (Figure 4d). Negative Eu resulted from plagioclase-feldspar fractionation along with low Sr content (ranging from 114 to 197 ppm with an average of 149.4 ppm). The main carriers of REEs in most shales are the accessory minerals such as monazite, zircon, apatite, xenotime and titanite, and plagioclase in the case of Eu [28] would therefore be a fractionation of accessory minerals can lead to a reduction in REEs content.

5. Discussion

5.1 Geochemical Classifications

The clastic sedimentary rocks or sediments can be classified on their geochemical composition. Various authors have proposed a very few of such classification schemes [38], [39], [40], [41]. The concentration ratio of SiO_2 and SiO_2/Al_2O_3 are the most commonly used geochemical criteria to describe sediment maturity [42] which also reflect the abundance of quartz, feldspar and clay contents in the sediments. The alkali content (Na_2O+K_2O) is also suitable as an index of chemical maturity and also serves as a measure of the feldspar content. Pettijohn [38] has proposed a geochemical classification for terrigenous sedimentary rocks based on a plot of log (Na_2O/K_2O) vs. log (SiO_2/Al_2O_3) by using an index of chemical maturity and the Na_2O/K_2O ratio. Based on this scheme, the studied sediments are predominantly sub-arkose with few sub-litharenites (Figure 5a). It is very noteworthy that the ternary diagram (Fe_2O_3(T)+MgO)-Na_2O- K_2O [40] also shows arkose distributions of the studied shale (Fig. 5b). Based on the Co-Th diagram of Hastie [43], all samples examined occupied by calc-alkaline and shoshonite series which obviously exhibit strong calc-alkaline affinity with high potassium content and shoshonitic persodicity (Figure 5c). According to fieldwork and geochemical evidence, it is likely related to an earlier metasomatized mafic thick source in the lower crust that enriched in alkalis under CO_2-containing partial melting due to asthenosphere rising beneath an incomplete rift [44] for studied Shale. Th/Yb vs. Zr/Y diagram (figure 5d) was developed from Ross and Bedard [45] for assessing the discrimination of magmatic affinities of the studied samples. The diagram shows that all the studied samples fall in the calc-alkaline field.

5.2 Provenance

Major elements provide information on both rock composition of the original provenance and the effects of sedimentary processes, such as weathering and sorting [5]. Geochemical data and their various approaches are of great importance for the relevant origin delineation [11], [46], [47], [48], [49]. These aid to explain the properties of the source rocks and ultimately provide distinct styles of sedimentary history [50], [51]. It is to be noted that the ratios of SiO_2/Al_2O_3 (3.32 to 4.69 with an average of 3.72) of the studied shale are almost similar to those of UCC and K_2O/Na_2O (2.50 to 4.33 with an Average of 3.62) of the studied shale are higher ratios of UCC [11], [12], [27]. The scheme reflects that the studied shales originated primarily from crustal granite sources. The Al_2O_3/TiO_2 ratio of the studied shales ranges from 17.49 to 24.57 with an average of 21.12. Such higher Al_2O_3/TiO_2 values are thought to be originated mainly from felsic to intermediate rock sources [46], [52]. The Na_2O-K_2O bivariate diagram [41] (figure 6a) provides a quartz-rich character of the source sediments.

The triangular diagram of (CaO+MgO)-SiO_2/10-(Na_2O+K_2O) (Figure 6b) represents the most remarkable and precise image of the provenance, showing clear distance from the fields of ultramafic and mafic rocks but close to granite field, indicating a dominant felsic contribution (after Taylor and McLennan, 1985).

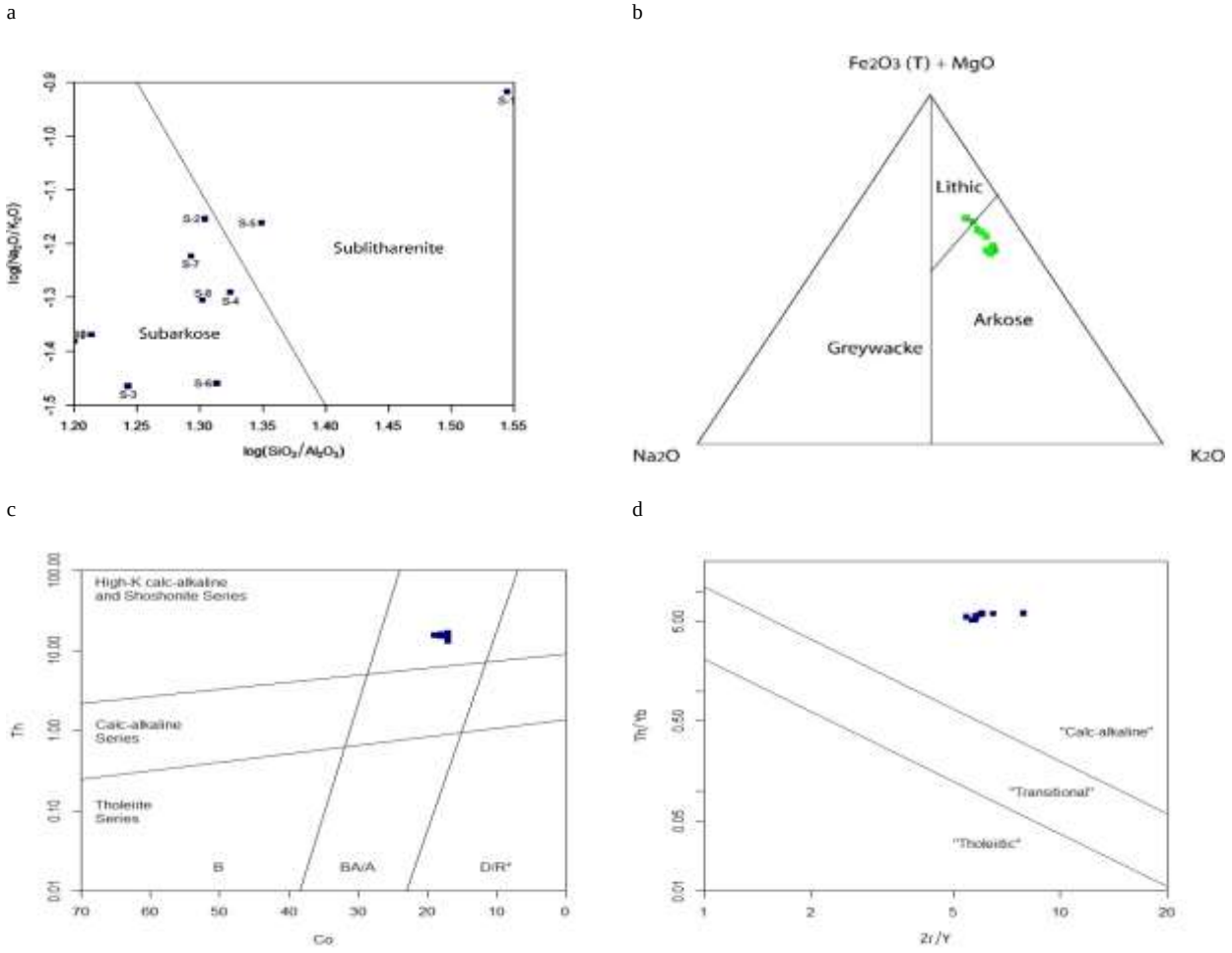

Fig. 5 - a) Geochemical classification diagrams; log (Na_2O/K_2O) vs. log (SiO_2/Al_2O_3) [38]**. b) (Fe_2O_3+MgO)-Na_2O-K_2O classification diagrams c) the Co-Th diagram** [43]**and d) Th/Yb vs. Zr/Y diagram for studied Shale for discrimination of magmatic affinities.**

The shales examined contain comparatively high K_2O and Rb concentrations. The ratio of K/Rb ratios of the studied shale ranges from 252.31 to 383.56 with an average of 320 close to the main trend with a ratio of 230 of a typical differentiated magmatic sequence (figure 6c), proposed by Shaw [53]. These results highlight the chemically coherent nature of the sediments and their origin mainly from acidic to intermediate rocks. On the other hand, zircon concentration is used to characterize the type and composition of the source rock [52], [54]. The low TiO_2/Zr ratios (33 to 45 with an average 41) of the sediments indicate felsic source rocks [46]. Hayashi [52] stated that TiO_2/Zr ratios allow the distinction between three different source rock types, such as felsic, intermediate and mafic rocks. The TiO_2 - Zr diagram (figure 6d) characterize the studied sediments from felsic source rocks[52].

The application of discriminant function analysis based on the composition of major elements or oxides in shales has been used to determine sediment provenance [55]. This discriminant function analysis distinguishes between four main fields of origin, namely mafic igneous rocks, intermediate igneous rocks, felsic igneous rocks and quartzose sedimentary rocks or recycled rocks. The discriminant functions are represented here as discriminant function 1 and discriminant function 2. The discriminant function 1 is the sum of (1.773 TiO_2), (0.607 Al_2O_3), (0.760 Fe_2O_3), (1.500 MgO), (0.616 CaO), (0.509 Na_2O), (1.224 K_2O) and (9.090), where Discriminant function 2 is the sum of (0.445 TiO_2), (0.070 Al_2O3), (0.250 Fe_2O_3), (1.142 MgO), (0.438 CaO), (1.475 Na_2O), (1.426 K_2O) and (-6.861). The discriminant function 1 of the studied shale ranges from -6.03 to -2.79 with an average of -4.33, while the discriminant function 2 ranges from -15.21 to -11.63 with an average of -13.78. According to the discriminant function diagram (figure 7), the shale samples are scattered in the quartzose sediment source field.

The bivariate plot of La/Th vs. Hf (Figure 8a) and the ternary plot of V-Ni-Th*10 (Figure 8.b) show that the studied shales have been derived from felsic source rocks.

Hiscott diagram (Figure 9a) allows distinction between ultramafic (UM), felsic metamorphic (ME) and granitic (GR) source composition [56]. The value of Y/Ni ratios (0.43-0.60 with an average 0.52) and the value of Cr/V ratios (0.99-1.11 with an average 1.06) are identical to the value of the sediments from the felsic source. This statement is also supported from the Th/Sc and Zr/Sc ratios diagram (Figure 9b).

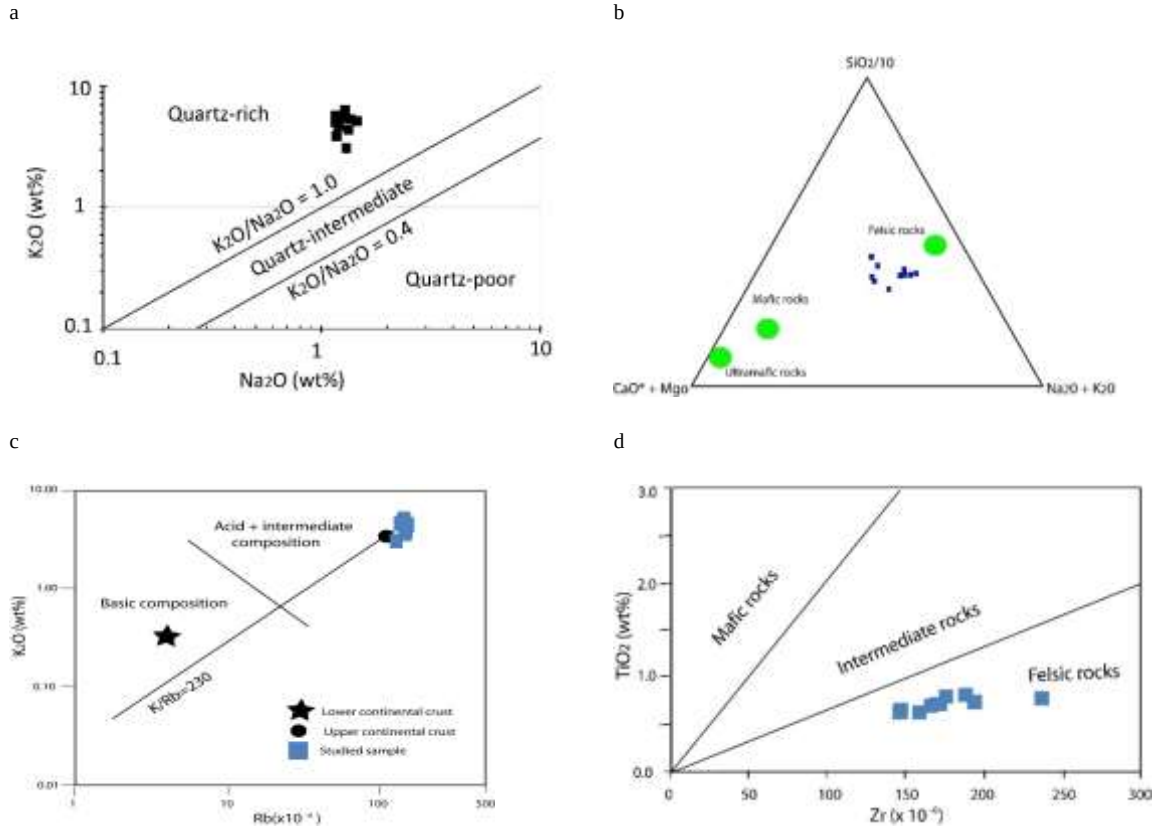

Fig. 6 - a) The bivariate plot of Na_2O- K_2O [41] **of the studied shale. b) The triangular diagram of (CaO+MgO)-SiO_2/10-(Na_2O+K_2O) c) Bivariate diagram of K_2O vs. Rb of the Neogene Shale of Zakiganj-1 well relative to a K/Rb ratio of 230** [53]**. d) TiO_2 - Zr diagram**

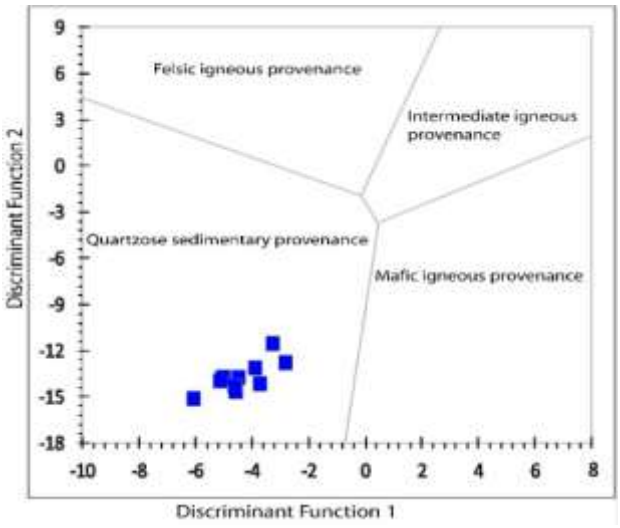

Fig. 7 - The discriminant function diagram shale samples

a b

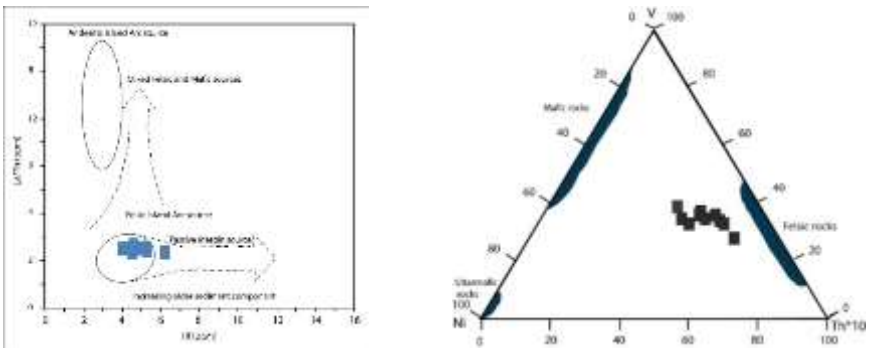

Fig. 8 - a) The bivariate diagram for La/Th versus Hf of the studied shale b) The ternary diagram for V-Ni-Th*10 of the studied shale.

a b

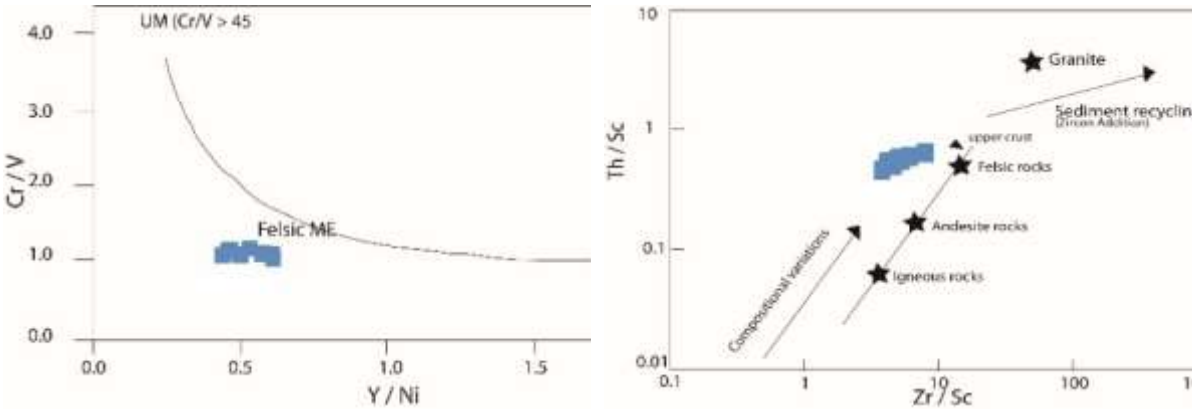

Fig. 9 - a) Hiscott Diagram (Cr/V vs. Y/Ni), allowing the discrimination between ultramafic (UM), felsic metamorphic (ME) and granitic (GR) source composition [56]**. b) Th/Sc and Zr/Sc ratios diagram showing the felsic source.**

5.3 Paleo Weathering of Source Area

Chemical weathering of rock materials led to the formation of clay minerals. Chemical weathering largely removes Ca, Na and K from the source rocks, and the amount of these elements surviving in the sediments derived from the rocks has served as an indicator of the intensity of chemical weathering [57]. The intensity of chemical weathering of source rocks is mainly controlled by the composition of the source rock, the duration of weathering, the climatic conditions and the rate of tectonic uplift of the source region [58]. About 75% of the labile materials in the upper crust consist of feldspars and volcanic glass [9], [59], [60], [61]. If siliciclastic sedimentary rocks are free of alkali related modifications after deposition, their alkali content (K_2O+Na_2O) and K_2O/Na_2O ratio should be considered as reliable indicators of the intensity of weathering of the parent material [62]. For determining the degree of weathering of the parent rock, some weathering indices based on the molecular proportions of mobile and immobile elements (Na_2O, CaO, K_2O and Al_2O_3) have been proposed. Therefore, the chemical composition of weathering products in a sedimentary environment is anticipated to provide information regarding the mobility of different elements during weathering phase [63]. The Chemical Index of Alteration (CIA), the Plagioclase Index of Alteration (PIA) and the Chemical Index of Weathering (CIW) are included in the weathering/alteration indices. The CIA proposed by Nesbitt and Young [64] is the most commonly used chemical index to determine the degree of weathering of the source area. They defined the CIA formula for evaluating the degree of chemical weathering as follows:

$$CIA = \frac{Al_2O_3}{(Al_2O_3 + CaO^* + Na_2O + K_2O} X100 \quad (1)$$

Where the CaO* is the CaO content contained in the silicate fraction.

CIA values range from almost 50 for fresh rock to 100 for completely weathered rock which provides a measure of the ratio of original/primary minerals and secondary products such as clay minerals. Therefore, CIA values increase with increasing weathering intensity and reach 100 when all Ca, Na and K have been leached from the weathering residues. The CIA values in the studied shale samples range between 61.32 and 70.54 with an average 66.90. The CIA indicated relatively moderate to high levels of chemical weathering in the source area. In addition to the CIA, the Chemical Index of Weathering (CIW) also provides information about the intensity of chemical weathering to which the sediments were exposed. Compared to other weathering indices,

the CIW is a superior method that includes a limited number of known components with consistent geochemical behavior during weathering. The CIW formula, expressed by Harnois [65] is as follows:

$$CIA = \frac{Al_2O_3}{(Al_2O_3 + CaO^* + Na_2O} X100 \quad (2)$$

Where the CaO* is the CaO content contained in the silicate fraction.

The CIW values of the studied Neogene Shale samples range from 80.48 to 89.43 with an average 84.48. These CIW values indicate moderate to high intensity chemical weathering. PIA monitors and quantifies the progressive weathering of feldspars into clay minerals.

The paleo weathering of source area and elemental redistribution during diagenesis can also be evaluated using the PIA [61]. The maximum PIA value is 100 for fully altered materials (i.e., kaolinite and gibbsite), and weathered plagioclase has a PIA value of 50. Fedo [61] defined the PIA formula for evaluating the extent of chemical weathering as follows:

$$CIA = \frac{(Al_2O_3 - K_2O)}{(Al_2O_3 + CaO^* + Na_2O - K_2O} X100 \quad (3)$$

The PIA values of the studied shale samples range from 71.83 to 85.29 with an average 78.97. Also, the PIA values indicate moderate to severe destruction of the feldspars during source weathering, transport, sedimentation and diagenesis. In the initial phase of weathering, Ca is washed out more quickly than Na and K. As weathering increases, the total alkali content (K_2O+Na_2O) decreases as the K-Na ratio (K_2O/Na_2O) increases. This is owing to the destruction of feldspars, from which plagioclase is removed better than potassium feldspars [59]. Feldspar materials in the shales were exposed to varying degrees of weathering during the different stages of development. The individual bivariate diagram of K_2O/Na_2O, K_2O+Na_2O, Na_2O, K_2O, and CaO vs. PIA can be used to elucidate the mobility of elements during the final stage of chemical weathering of previously altered feldspars. In the bivariate diagram of K_2O/Na_2O vs. PIA and K_2O+Na_2O vs. PIA (figures 10a, b), the values of K_2O/Na_2O and the total alkali content in most samples decreases with increasing PIA value. Figures 11a, 11b and 11c show the decreasing trend of Na, Ca and K with increasing of PIA which reflect the behavior of Na, Ca and K during the progressive weathering of feldspars in the shales.

The ternary diagram of A-CN-K proposed by [59] is another method that can be used to the composition of the original source rock as well as the mobility of elements during the process of chemical weathering of the source material and after deposition chemical modifications. The ternary diagram of Al_2O_3-($CaO+Na_2O$)-K_2O (represented as A-CN-K) is useful for identifying compositional changes of shales associated with chemical weathering, diagenesis and source rock composition. Geochemical data of the Neogene shales from Zakiganj-1 well site was presented in an A-CN-K diagram (figure 12). Arrows 1 to 5 represent the weathering trends of gabbro, tonalite, granodiorite, adamellite and granite, respectively [66]. In the A-CN-K diagram (figure 12), the shales are plotted above the line connecting plagioclase and potassium feldspar. The diagrams define a narrow linear trend that runs slightly obliquely parallel to the A-CN edge. This may be due to the fact that the removal rate of Na and Ca from plagioclase is generally greater than the removal rate of K from microcline [59]. The plot trends toward illite on the A-K edge and shows no bias toward the K tip, suggesting that the shales are free of potassium metasomatization during diagenesis. If the trend line is extended backwards, it intersects the plagioclase-potassium feldspar connection near arrow 5, which is the granite field (potential final source). The linear weathering trend indicates a stable state of weathering conditions where material removal coincides with the production of weathering material [57].

a b

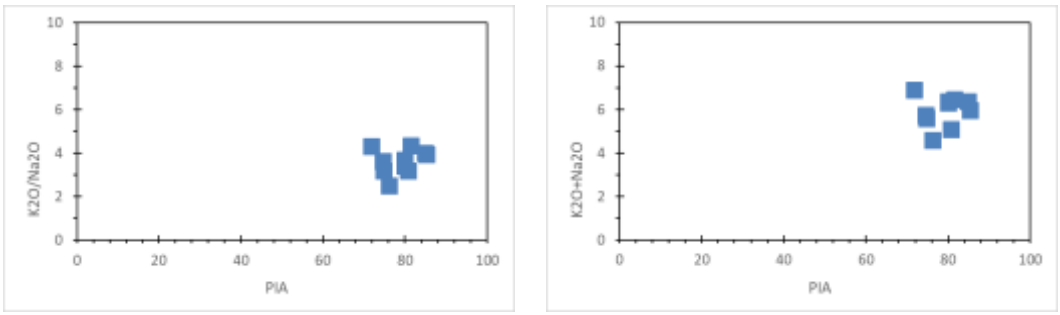

Fig. 10 - Bivariate plots depicting the mobility of elements during weathering of feldspars in the shale samples of (a) (K_2O/Na_2O) wt. % versus PIA. (b) ($K_2O + Na_2O$) wt% versus PIA.

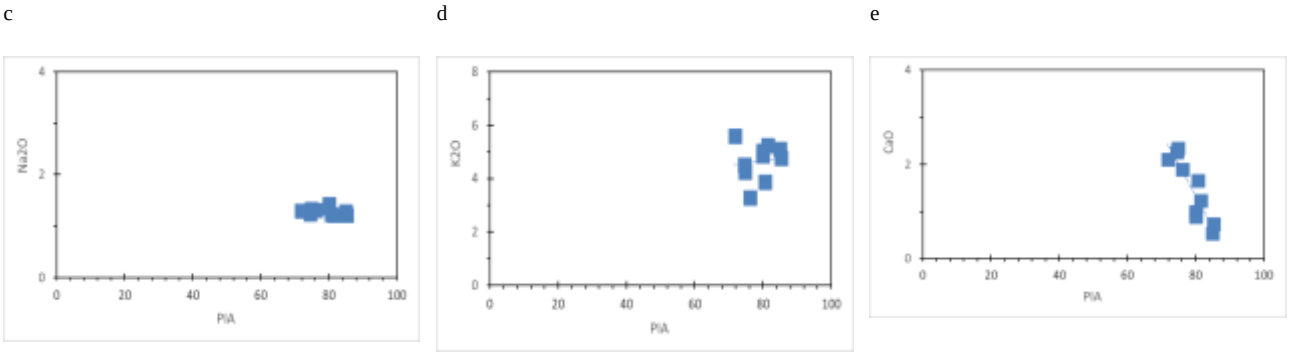

Fig. 11 - Bivariate plots depicting the mobility of elements during weathering of feldspars in the shale samples of (a) Na_2O wt. % versus PIA. (b) CaO wt. % versus PIA. (c) K_2O wt. % versus PIA.

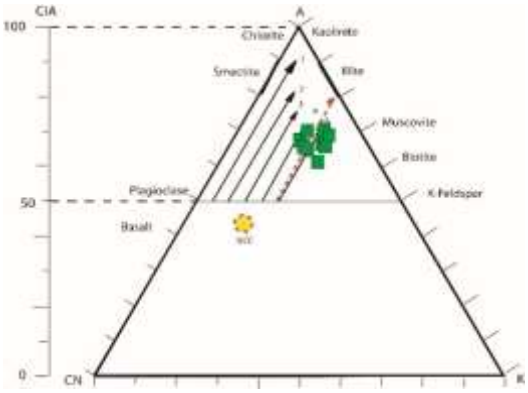

Fig. 12 - A-CN-K ternary diagram of the molecular fractions of Al_2O_3 -(CaO+Na_2O)-K_2O for shale samples from Zakiganj-1 well, the dashed arrow shows the original weathering trend for the shale samples (the CIA scale is also shown at the left side is for comparison).

5.4 Climatic Condition, Sediment Maturity and Redox Condition

The index compositional variation (ICV) proposed by [67] is used to the original nature and maturity of sediments as well as the prevailing climatic conditions. The ICV seems to be highest for minerals with high weathering intensity and decreases for more stable minerals (less weathered minerals). The ICV further decreases for the clay minerals of the montmorillonite (smectite) group and is lowest for the minerals of the kaolinite group [67]. Additionally, more mature shale tends to have low ICV values (<1.0). The ICV is calculated as

$$ICV = \frac{(Fe_2O_3 + K_2O + Na_2O + CaO + MgO + MnO)}{Al_2O_3} \quad (4)$$

Shales with an ICV>1 are compositionally immature because the first sedimentary cycle was deposited in tectonically active environments [67]. On the contrary, sediments with ICV<1 are compositionally mature. For this case the sediments were deposited in the tectonically quiescent or cratonic environment where sediment recycling was active. For the studied shales, the ICV values range from 0.87 to 1.10 with an average 0.95 [only one sample (S6) show ICV >1 (1.10)]. Based on the average ICV values, it can be concluded that the shale composition is mature and deposited in the tectonically quiescent or cratonic environment. The K_2O/Na_2O ratios vary from 2.5 to 4.33 with an average 3.62 for the studied shale samples. These ratios indicated moderate to high maturity of the shales, which is consistent with the ICV values [58]. The binary plot of CIA vs. ICV for the studied samples (figure 13a) shows that all the shales are geochemically mature except sample S-6. All the studied shales have come from weakly weathered source rocks and are very close to UCC and PASS. Alternatively, the SiO_2/Al_2O_3 ratios of siliciclastic rocks are sensitive to sediment recycling and weathering processes and can serve as an indicator of sediment maturity. As sediment matures, quartz survives preferentially over feldspars, mafic minerals and lithics [3], [68]. The SiO_2/Al_2O_3 ratios in unaltered igneous rocks are between 3.0 (basic rocks) and 5.0 (acidic rocks). Values of the SiO_2/Al_2O_3 ratio in the studied shales range from 3.32 to 4.69 with an average 3.72 indicate that the shales are basic to acidic rocks. The K_2O/Na_2O ratios of the shales vary from 2.50 to 4.33 with an average 3.62. The low values of K_2O/Na_2O and the Low to moderate values of SiO_2/Al_2O_3 indicate moderate to high sediment maturity. The climatic conditions during the sedimentation of siliciclastic sedimentary rocks can be assessed by the plot of SiO_2 vs. (Al_2O_3+K_2O+Na_2O) proposed by [69] was used to estimate the maturity of studied shales as a function of climate to classify. Figure 13b shows that most shales occur in the semi-arid climate region with different degrees of maturity.

The redox state is very important for detecting sediment deposition in marine or non-marine environments. Furthermore, the accumulation of certain trace metals in sediments is directly or indirectly controlled by redox conditions, either through a change in redox state and/or through speciation [70]. The

studied shales have a minimum V content of 100 to a maximum V content of 117 ppm with an average of 106.9 ppm and a Ni content of a minimum of 50 ppm to a maximum of 60 ppm with an average of 56 ppm. The solubility of vanadium in natural waters, its extraction from seawater and its absorption in sediments are mainly influenced by redox conditions [71]. During early diagenetic alteration of sediments, V tends to mobilize from the biogenic materials in oxic environments, whereas the mobilization of V is very limited under anoxic conditions [72]. Furthermore, Ni is mainly enriched in organic-rich sediments where these metals are intercalated with organic material [73], [74]. The proportionality of these two elements V/(V+Ni) is very important to derive information about Eh, pH and sulfide activity in the depositional environment [75]. The Neogene shales from the Zakiganj-1 well have low V/(V+Ni) ratios range from 0.63 to 0.68 with an average 0.66. The V/(V+Ni) ratios are below 0.8, indicating the moderate abundance in the redox state of the depositional environment. The Ni/Co ratio is also a redox indicator [76], [77], [78]. Jones and Manning (1994) suggested that Ni/Co ratios below 5 indicate oxic environments, while ratios above 5 indicate sub-oxic and anoxic environments[79]. The Neogene shales from the Zakiganj-1 well range from 2.78 to 3.53 with an average 3.18, suggesting that these sediments were deposited in oxic environments.

5.5 Tectonic Settings

Siliciclastic rocks from different tectonic environments possess terrain-specific geochemical signatures. Several researchers have mentioned that the chemical composition of siliciclastic sedimentary rocks is largely controlled by the plate tectonic conditions of their origin and deposition basins[1], [2], [55]. Tectonic setting discrimination diagrams give consistent results for siliciclastic rocks that have not been deeply influenced by post-depositional weathering and metamorphism [5]. Bivariate plots of the major and trace element geochemistry have been used by several researchers to determine the tectonic nature of shales [1], [2], [55][80], [81], [82]. Among the various discrimination diagrams for tectonic settings, the major elements/oxides based discrimination diagrams of Taylor and McLennan [11] and Bhatia[1] are often used. Bhatia[1] has divided series of tectonic diagrams to distinguish among the four main tectonic areas. These are namely the oceanic island arc (OIA), the continental island arc (CIA), the active continental margin (ACM) as well as the passive continental margin (PM).

Chemical analysis data of the studied shales were presented in four diagrams to notice the tectonic settings. Bivariate diagram of TiO_2 vs. (Fe_2O_3+MgO) reveals that all samples were belongs to the continental island arc (CIA) field. The Al_2O_3/SiO_2 vs. Fe_2O_3+MgO reveals that most of the studied samples were plotted in the oceanic island arc (OIA) fields (figures 14 a and 14b).

All the shale samples represent the active continental margin field (figure 14c) on the K_2O/Na_2O vs. SiO_2 tectonic setting discrimination diagram. More detailed results can also be obtained using the calc-alkaline ternary diagram (CaO-Na_2O-K_2O). The calc-alkaline ternary diagram (figure 15a) exhibits that most shales samples are associated with the active continental margin. The rest are associated with the passive continental margin.

The Th-Sc-Zr/10 tectonic discrimination diagram [2] shown that the source area for most shale samples is located predominantly on the passive continental margin (figure 15b). The immobile elements such as La, Zr and Hf are enriched in the passive edge setting[1], [2], [55]. The La-Th-Sc tectonic distinction diagram shows the active and passive margin setting of the depositional basin for the studied shales (figure 15c).

a b

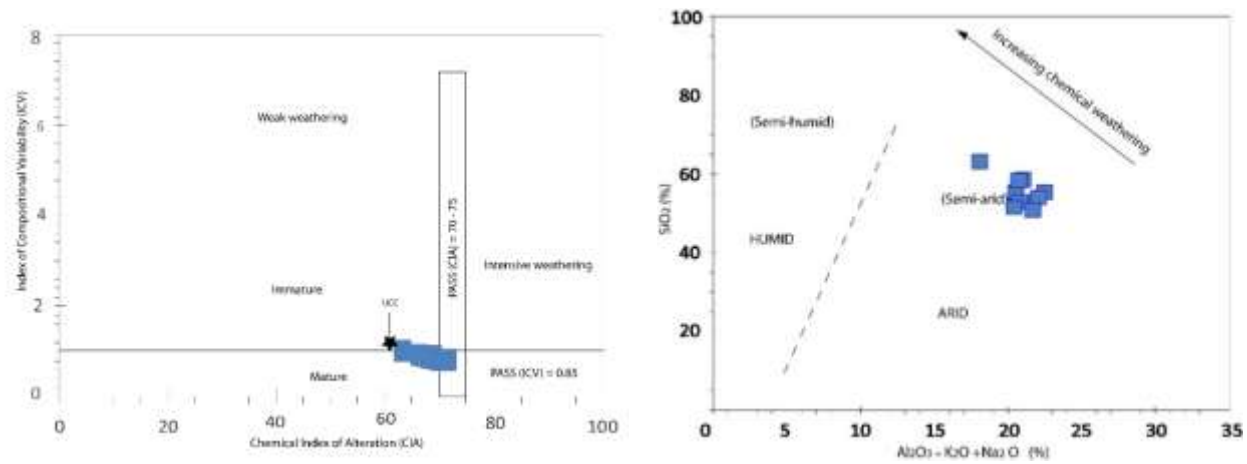

Fig. 13 - The binary plot of (a) CIA versus ICV for the studied samples and (b) SiO_2 versus (Al_2O_3 + K_2O + Na_2O) [69] **to estimate the maturity of studied shales as a function of climate to classify.**

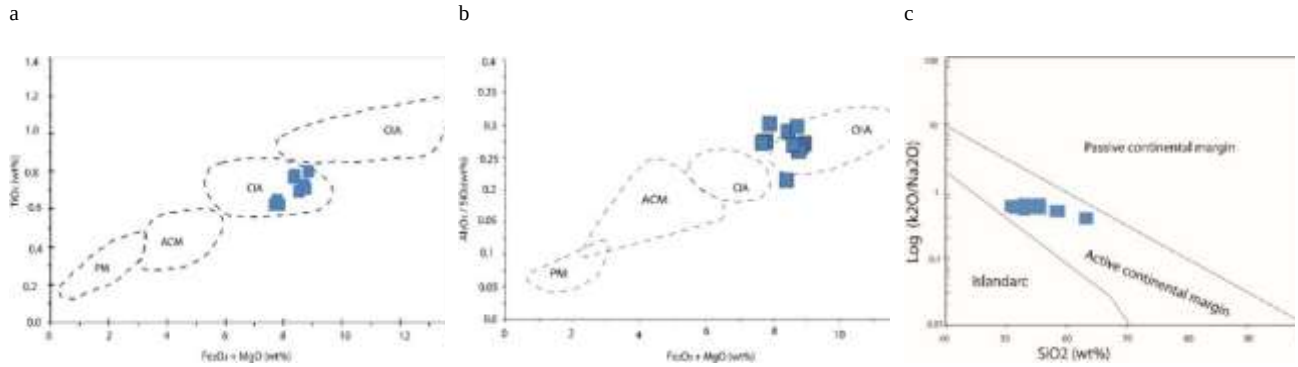

Fig. 14 – (a) Bivariate diagram of TiO_2 versus (Fe_2O_3 + MgO) (b) The bivariate diagram of Al_2O_3/SiO_2 versus Fe_2O_3 + MgO (c) The K_2O/Na_2O versus SiO_2 tectonic-setting discrimination diagram.

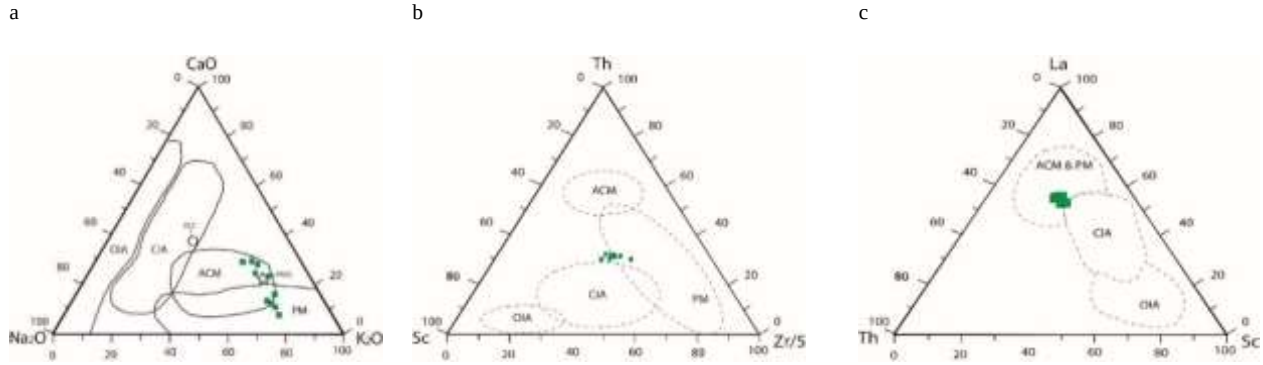

Fig. 15 – (a) The calc-alkaline ternary diagram (CaO-Na_2O-K_2O) (b) The Th-Sc-Zr/10 tectonic discrimination diagram[2] **and c) The La-Th-Sc tectonic distinction diagram.**

6. Conclusions

Important information about the composition, tectonic setting and evolution of the continental crust can easily be obtained from clastic sediments. Their chemical records are influenced by factors such as parent rock properties, climate, chemical weathering, and sorting processes during transport, sedimentation, and post depositional diagenesis. The Neogene shales from the Zakiganj-1 well mostly exhibit greater variations in the geochemistry of their major elements, reflecting the unstable conditions of provenance and tectonic setting. The geochemical classification of the Neogene Shales of Zakiganj-1 well shows akrose group mainly sub-arkose with only one sub-litharenites. All samples show calc-alkaline affinities. Some major and trace elements show an obvious positive correlation with Al_2O_3, confirming a clear hydraulic fractionation. The ratio of SiO_2/Al_2O_3 (average 3.72) of the studied shale are almost similar to those of UCC and reflects that the studied shales originated primarily from crustal granite sources. Most of the geochemical data indicate primarily the felsic igneous provenance types but discrimination diagrams show the continental signature derivatives, consisting primarily of quartz-rich sediments and quartzose sedimentary provenance. Therefore, the sediments could originate from both felsic igneous rocks and quartzose sedimentary sources. The CIA value (average 66.90) and CIW value (average 84.48) indicate moderate to high intensity chemical weathering. The ICV (<1), K2O/Na2O ratios (average 3.62) and PIA values (average 78.97) show moderate to high maturity levels and moderate to severe destruction of the feldspars during source weathering, transport, sedimentation and diagenesis. The lower ratios of V/(V+Ni) and Ni/Co indicate the moderate abundance in the redox state of the oxic depositional environment. Based on the distinction between major and trace elements, the tectonic settings were typically delineated as active and passive margin of provenance setting.

Acknowledgements

Many thanks to the Director General and the Director (Administration and Training) of Bangladesh Petroleum Institute (BPI) for the organizational and financial support. The authors would like to thank the editors and anonymous reviewers for their constructive comments, which really help to improve the manuscript. We thank Chairman of Petrobangla and Managing Director of BAPEX for their warm support in collection of samples and data.

References

[1] M. R. Bhatia, “Plate tectonics and geochemical composition of sandstones.,” *J. Geol.*, vol. 91, no. 6, pp. 611–627, Nov. 1983, doi: 10.1086/628815.

[2] M. R. Bhatia and K. A. W. Crook, "Trace element characteristics of graywackes and tectonic setting discrimination of sedimentary basins," *Contrib. to Mineral. Petrol.*, vol. 92, no. 2, pp. 181–193, 1986.

[3] B. P. Roser and R. J. Korsch, "Determination of Tectonic Setting of Sandstone-Mudstone Suites Using SiO 2 Content and K 2 O/Na 2 O Ratio," *J. Geol.*, vol. 94, no. 5, pp. 635–650, Sep. 1986, doi: 10.1086/629071.

[4] B. P. Roser and R. J. Korsch, "Provenance signatures of sandstone-mudstone suites determined using discriminant function analysis of major-element data," *Chem. Geol.*, vol. 67, no. 1–2, pp. 119–139, Jan. 1988, doi: 10.1016/0009-2541(88)90010-1.

[5] S. M. McLennan, S. Hemming, D. K. McDaniel, and G. N. Hanson, "Geochemical approaches to sedimentation, provenance, and tectonics," *Spec. Pap. Geol. Soc. Am.*, vol. 284, pp. 21–40, 1993, doi: 10.1130/SPE284-p21.

[6] H. W. Nesbitt, G. M. Young, S. M. McLennan, and R. R. Keays, "Effects of Chemical Weathering and Sorting on the Petrogenesis of Siliciclastic Sediments, with Implications for Provenance Studies," *J. Geol.*, vol. 104, no. 5, pp. 525–542, Sep. 1996, doi: 10.1086/629850.

[7] L. Bracciali, M. Marroni, P. Luca, and R. Sergio, "Geochemistry and petrography of Western Tethys Cretaceous sedimentary covers (Corsica and Northern Apennines): From source areas to configuration of margins," in *Sedimentary Provenance and Petrogenesis: Perspectives from Petrography and Geochemistry*, Geological Society of America, 2007. doi: 10.1130/2006.2420(06).

[8] J. J. Veevers, "Earth's paleoclimate and sedimentary environments," *Pangea Paleoclimate, tectonics, Sediment. Dur. accretion, zenith, Break. a supercontinent*, vol. 288, p. 13, 1994.

[9] S. R. Taylor and S. M. McLennan, "The continental crust: its composition and evolution," 1985.

[10] Y. Yan *et al.*, "Geochemistry of the sedimentary rocks from the Nanxiong Basin, South China and implications for provenance, paleoenvironment and paleoclimate at the K/T boundary," *Sediment. Geol.*, vol. 197, no. 1–2, pp. 127–140, Apr. 2007, doi: 10.1016/j.sedgeo.2006.09.004.

[11] S. R. Tylor and S. M. McLennan, "The continental crust: its composition and evolution, An examination of the geochemical record preserved in sediementary rocks." Blackwell Scientific Publications, 1985.

[12] K. C. Condie, "Chemical composition and evolution of the upper continental crust: Contrasting results from surface samples and shales," *Chem. Geol.*, vol. 104, no. 1–4, pp. 1–37, Feb. 1993, doi: 10.1016/0009-2541(93)90140-E.

[13] S. . McLennan, A. Simonetti, and S. . Goldstein, "Nd and Pb isotopic evidence for provenance and post-depositional alteration of the Paleoproterozoic Huronian Supergroup, Canada," *Precambrian Res.*, vol. 102, no. 3–4, pp. 263–278, Aug. 2000, doi: 10.1016/S0301-9268(00)00070-X.

[14] K. C. Condie, "Another look at rare earth elements in shales," *Geochim. Cosmochim. Acta*, vol. 55, no. 9, pp. 2527–2531, Sep. 1991, doi: 10.1016/0016-7037(91)90370-K.

[15] D. J. Wronkiewicz and K. C. Condie, "Geochemistry and mineralogy of sediments from the Ventersdorp and Transvaal Supergroups, South Africa: Cratonic evolution during the early Proterozoic," *Geochim. Cosmochim. Acta*, vol. 54, no. 2, pp. 343–354, Feb. 1990, doi: 10.1016/0016-7037(90)90323-D.

[16] M. J. J. Rahman and P. Faupl, "The composition of the subsurface Neogene shales of the Surma group from the Sylhet Trough, Bengal Basin, Bangladesh," *Sediment. Geol.*, vol. 155, no. 3–4, pp. 407–417, 2003.

[17] M. J. J. Rahman and S. Suzuki, "Composition of Neogene shales from the Surma Group, Bengal Basin, Bangladesh: Implications for provenance and tectonic setting," *Austrian Jour. Earth Sci*, vol. 100, pp. 54–64, 2007.

[18] M. M. Alam, M. R. Islam, and M. A. I. Khan, "Geological analysis of Zakiganj Upazila and feasibility study of available geo resources," *Am J Min Met.*, vol. 2, no. 3, pp. 46–50, 2014.

[19] K. Hiller and M. Elahi, "Structural development and hydrocarbon entrapment in the Surma basin/Bangladesh (northwest Indo Burman fold belt)," in *SPE Offshore South East Asia Show*, SPE, 1984, p. SPE-12398.

[20] S. Y. Johnson and A. B. U. M. D. NUR ALAM, "Sedimentation and tectonics of the Sylhet trough, Bangladesh," *Geol. Soc. Am. Bull.*, vol. 103, no. 11, pp. 1513–1527, 1991.

[21] J. F. Holtrop and J. Keizer, "Some aspects of the stratigraphy and correlation of the Surma Basin wells, East Pakistan," *ECAFE Miner. Resour. Dev. Ser.*, vol. 36, pp. 143–154, 1970.

[22] M. A. M. Khan, M. Ismail, and M. Ahmad, "Geology and hydrocarbon prospects of the Surma Basin, Bangladesh," 1988.

[23] H.-U. Worm *et al.*, "Large sedimentation rate in the Bengal delta: magnetostratigraphic dating of Cenozoic sediments from northeastern Bangladesh," *Geology*, vol. 26, no. 6, pp. 487–490, 1998.

[24] K. K. Turekian and K. H. Wedepohl, "Distribution of the elements in some major units of the earth's crust," *Geol. Soc. Am. Bull.*, vol. 72, no. 2, pp. 175–192, 1961.

[25] M. P. Dabard, "Lower Brioverian formations (Upper Proterozoic) of the Armorican Massif (France): geodynamic evolution of source areas revealed by sandstone petrography and geochemistry," *Sediment. Geol.*, vol. 69, no. 1–2, pp. 45–58, Nov. 1990, doi: 10.1016/0037-0738(90)90100-8.

[26] S. M. McLennan, "Relationships between the trace element composition of sedimentary rocks and upper continental crust," *Geochemistry, Geophys. Geosystems*, vol. 2, no. 4, Apr. 2001, doi: 10.1029/2000GC000109.

[27] R. L. Rudnick and S. Gao, "Composition of the Continental Crust," *Treatise on Geochemistry*, vol. 3–9, pp. 1–64, 2003, doi: 10.1016/B0-08-043751-6/03016-4.

[28] L. P. Gromet and L. T. Silver, "Rare earth element distributions among minerals in a granodiorite and their petrogenetic implications," *Geochim. Cosmochim. Acta*, vol. 47, no. 5, pp. 925–939, 1983.

[29] F. J. Pettijohn, *Sedimentary rocks*, vol. 3. Harper & Row New York, 1975.

[30] C. Baiyegunhi, K. Liu, and O. Gwavava, "Geochemistry of sandstones and shales from the Ecca Group, Karoo Supergroup, in the Eastern Cape Province of South Africa: Implications for provenance, weathering and tectonic setting," *Open Geosci.*, vol. 9, no. 1, Aug. 2017, doi: 10.1515/geo-2017-0028.

[31] D. K. Roy and B. P. Roser, "Geochemistry of Tertiary sequence in Shahbajpur-1 well, Hatia trough, Bengal basin, Bangladesh: provenance, source weathering and province affinity," *J. Life Earth Sci.*, vol. 7, pp. 1–13, 2012.

[32] F. J. Pettijohn, "Paleocurrents of Lake Superior Precambrian quartzites," *Bull. Geol. Soc. Am.*, vol. 68, no. 4, pp. 469–480, 1957, doi: 10.1130/0016-7606(1957)68[469:POLSPQ]2.0.CO;2.

[33] B. K. Das, A. S. AL-Mikhlafi, and P. Kaur, "Geochemistry of Mansar Lake sediments, Jammu, India: Implication for source-area weathering, provenance, and tectonic setting," *J. Asian Earth Sci.*, vol. 26, no. 6, pp. 649–668, May 2006, doi: 10.1016/j.jseaes.2005.01.005.

[34] W. V Boynton, "Cosmochemistry of the rare earth elements: meteorite studies," in *Developments in geochemistry*, vol. 2, Elsevier, 1984, pp. 63–114.

[35] I. Hossain, K. K. Roy, P. K. Biswas, M. Alam, M. Moniruzzaman, and F. Deeba, "Geochemical characteristics of Holocene sediments from Chuadanga district, Bangladesh: implications for weathering, climate, redox conditions, provenance and tectonic setting," *Chinese J. Geochemistry*, vol. 33, pp. 336–350, 2014.

[36] B. Bauluz, M. J. Mayayo, C. Fernandez-Nieto, and J. M. G. Lopez, "Geochemistry of Precambrian and Paleozoic siliciclastic rocks from the Iberian Range (NE Spain): implications for source-area weathering, sorting, provenance, and tectonic setting.," *Chem. Geol.*, vol. 168, no. 1–2, pp. 135–150, 2000.

[37] P. Henderson, *The rare earth elements: introduction and review; in Jones, A.P., Wall, F., Williams, C.T., eds., Rare Earth Minerals; Chemistry, Origin and Ore deposits*, vol. 7. 1996.

[38] F. J. Pettijohn, P. E. Potter, and R. Siever, "Sand and sandstone. Plate motions inferred from major element chemistry of lutites," *Precambrian Res.*, vol. 147, pp. 124–147, 1972.

[39] M. M. Herron, "Geochemical classification of terrigenous sands and shales from core or log data," *J. Sediment. Res.*, vol. 58, no. 5, pp. 820–829, 1988.

[40] H. Blatt, G. V Middleton, and R. C. Murray, "Origin of sedimentary rocks," *(No Title)*, 1980.

[41] K. A. W. Crook, "Lithogenesis and geotectonics: the significance of compositional variation in flysch arenites (graywackes)," 1974.

[42] P. E. Potter, "Petrology and chemistry of modern big river sands," *J. Geol.*, vol. 86, no. 4, pp. 423–449, 1978.

[43] A. R. Hastie, A. C. Kerr, J. A. Pearce, and S. F. Mitchell, "Classification of altered volcanic island arc rocks using immobile trace elements: development of the Th–Co discrimination diagram," *J. Petrol.*, vol. 48, no. 12, pp. 2341–2357, 2007.

[44] M. L. Renjith *et al.*, "Zircon U–Pb age, Lu–Hf isotope, mineral chemistry and geochemistry of Sundamalai peralkaline pluton from the Salem Block, southern India: Implications for Cryogenian adakite-like magmatism in an aborted-rift," *J. Asian Earth Sci.*, vol. 115, pp. 321–344, 2016.

[45] P.-S. Ross and J. H. Bédard, "Magmatic affinity of modern and ancient subalkaline volcanic rocks determined from trace-element discriminant diagrams," *Can. J. Earth Sci.*, vol. 46, no. 11, pp. 823–839, 2009.

[46] Ş. Keskin, "Geochemistry of Çamardı Formation sediments, central Anatolia (Turkey): implication of source area weathering, provenance, and tectonic setting," *Geosci. J.*, vol. 15, pp. 185–195, 2011.

[47] J. S. Armstrong-Altrin, Y. Il Lee, S. P. Verma, and S. Ramasamy, "Geochemistry of sandstones from the Upper Miocene Kudankulam Formation, southern India: implications for provenance, weathering, and tectonic setting," *J. Sediment. Res.*, vol. 74, no. 2, pp. 285–297, 2004.

[48] R. L. Cullers, "The controls on the major-and trace-element evolution of shales, siltstones and sandstones of Ordovician to Tertiary age in the Wet Mountains region, Colorado, USA," *Chem. Geol.*, vol. 123, no. 1–4, pp. 107–131, 1995.

[49] K. C. Condie, M. D. Boryta, J. Liu, and X. Qian, "The origin of khondalites: geochemical evidence from the Archean to Early Proterozoic granulite belt in the North China craton," *Precambrian Res.*, vol. 59, no. 3–4, pp. 207–223, 1992.

[50] W. R. Dickinson, "Interpreting provenance relations from detrital modes of sandstones," in *Provenance of arenites*, Springer, 1985, pp. 333–361.

[51] W. R. Dickinson, "Provenance and sediment dispersal in relation to paleotectonics and paleogeography of sedimentary basins," in *New perspectives in basin analysis*, Springer, 1988, pp. 3–25.

[52] K.-I. Hayashi, H. Fujisawa, H. D. Holland, and H. Ohmoto, "Geochemistry of~ 1.9 Ga sedimentary rocks from northeastern Labrador, Canada," *Geochim. Cosmochim. Acta*, vol. 61, no. 19, pp. 4115–4137, 1997.

[53] D. M. Shaw, "A review of K-Rb fractionation trends by covariance analysis," *Geochim. Cosmochim. Acta*, vol. 32, no. 6, pp. 573–601, 1968.

[54] S. Paikaray, S. Banerjee, and S. Mukherji, "Geochemistry of shales from the Paleoproterozoic to Neoproterozoic Vindhyan Supergroup: Implications on provenance, tectonics and paleoweathering," *J. Asian Earth Sci.*, vol. 32, no. 1, pp. 34–48, 2008.

[55] B. P. Roser and R. J. Korsch, "Determination of tectonic setting of sandstone-mudstone suites using SiO2 content and K2O/Na2O ratio," *J. Geol.*, vol. 94, no. 5, pp. 635–650, 1986.

[56] R. N. Hiscott, "Ophiolitic source rocks for Taconic-age flysch: trace-element evidence," *Geol. Soc. Am. Bull.*, vol. 95, no. 11, pp. 1261–1267, 1984.

[57] H. W. Nesbitt, C. M. Fedo, and G. M. Young, "Quartz and Feldspar Stability, Steady and Non-Steady-State Weathering, and Petrogenesis of Siliciclastic Sands and Muds," *J. Geol.*, vol. 105, no. 2, pp. 173–192, Mar. 1997, doi: 10.1086/515908.

[58] D. J. Wronkiewicz and K. C. Condie, "Geochemistry of Archean shales from the Witwatersrand Supergroup, South Africa: Source-area weathering and provenance," *Geochim. Cosmochim. Acta*, vol. 51, no. 9, pp. 2401–2416, Sep. 1987, doi: 10.1016/0016-7037(87)90293-6.

[59] H. . Nesbitt and G. . Young, "Prediction of some weathering trends of plutonic and volcanic rocks based on thermodynamic and kinetic considerations," *Geochim. Cosmochim. Acta*, vol. 48, no. 7, pp. 1523–1534, Jul. 1984, doi: 10.1016/0016-7037(84)90408-3.

[60] H. W. Nesbitt and G. M. Young, "Formation and Diagenesis of Weathering Profiles," *J. Geol.*, vol. 97, no. 2, pp. 129–147, Mar. 1989, doi: 10.1086/629290.

[61] C. M. Fedo, H. Wayne Nesbitt, and G. M. Young, "Unraveling the effects of potassium metasomatism in sedimentary rocks and paleosols, with implications for paleoweathering conditions and provenance," *Geology*, vol. 23, no. 10, pp. 921–924, 1995.

[62] D. A. Lindsey, "An evaluation of alternative chemical classifications of sandstones," US Geological Survey, 1999.

[63] K. P. Singh, "Nonlinear estimation of aquifer parameters from surficial resistivity measurements," *Hydrol. Earth Syst. Sci. Discuss.*, vol. 2, no. 3, pp. 917–938, 2005.

[64] Hw. Nesbitt and G. M. Young, "Early Proterozoic climates and plate motions inferred from major element chemistry of lutites," *Nature*, vol. 299, no. 5885, pp. 715–717, 1982.

[65] L. Harnois, "The CIW index: a new chemical index of weathering," *Sediment. Geol.*, vol. 55, no. 3, pp. 319–322, 1988.

[66] C. M. Fedo, G. M. Young, and H. W. Nesbitt, "Paleoclimatic control on the composition of the Paleoproterozoic Serpent Formation, Huronian Supergroup, Canada: a greenhouse to icehouse transition," *Precambrian Res.*, vol. 86, no. 3–4, pp. 201–223, 1997.

[67] R. Cox, D. R. Lowe, and R. L. Cullers, "The influence of sediment recycling and basement composition on evolution of mudrock chemistry in the southwestern United States," *Geochim. Cosmochim. Acta*, vol. 59, no. 14, pp. 2919–2940, 1995.

[68] B. P. Roser, R. A. Cooper, S. Nathan, and A. J. Tulloch, "Reconnaissance sandstone geochemistry, provenance, and tectonic setting of the lower Paleozoic terranes of the West Coast and Nelson, New Zealand," *New Zeal. J. Geol. Geophys.*, vol. 39, no. 1, pp. 1–16, 1996.

[69] L. J. Suttner and P. K. Dutta, "Alluvial sandstone composition and paleoclimate; I, Framework mineralogy," *J. Sediment. Res.*, vol. 56, no. 3, pp. 329–345, 1986.

[70] J. L. McKay, T. F. Pedersen, and A. Mucci, "Sedimentary redox conditions in continental margin sediments (NE Pacific)—Influence on the accumulation of redox-sensitive trace metals," *Chem. Geol.*, vol. 238, no. 3–4, pp. 180–196, 2007.

[71] A. Bellanca *et al.*, "Orbitally induced limestone/marlstone rhythms in the Albian—Cenomanian Cismon section (Venetian region, northern Italy): Sedimentology, calcareous and siliceous plankton distribution, elemental and isotope geochemistry," *Palaeogeogr. Palaeoclimatol. Palaeoecol.*, vol. 126, no. 3–4, pp. 227–260, 1996.

[72] T. J. Shaw, J. M. Gieskes, and R. A. Jahnke, "Early diagenesis in differing depositional environments: the response of transition metals in pore water," *Geochim. Cosmochim. Acta*, vol. 54, no. 5, pp. 1233–1246, 1990.

[73] J. S. Leventhal and J. W. Hosterman, "Chemical and mineralogical analysis of Devonian black-shale samples from Martin County, Kentucky; Carroll and Washington counties, Ohio; Wise County, Virginia; and Overton County, Tennessee, USA," *Chem. Geol.*, vol. 37, no. 3–4, pp. 239–264, 1982.

[74] M. Glikson, B. W. Chappell, R. S. Freeman, and E. Webber, "Trace elements in oil shales, their source and organic association with particular reference to Australian deposits," *Chem. Geol.*, vol. 53, no. 1–2, pp. 155–174, 1985.

[75] J. Madhavaraju and Y. Il Lee, "Geochemistry of the Dalmiapuram Formation of the Uttatur Group (Early Cretaceous), Cauvery basin, southeastern India: Implications on provenance and paleo-redox conditions," *Rev. Mex. ciencias geológicas*, vol. 26, no. 2, pp. 380–394, 2009.

[76] R. Nagarajan, J. Madhavaraju, R. Nagendra, J. S. Armstrong-Altrin, and J. Moutte, "Geochemistry of Neoproterozoic shales of the Rabanpalli Formation, Bhima Basin, Northern Karnataka, southern India: implications for provenance and paleoredox conditions," *Rev. Mex. ciencias geológicas*, vol. 24, no. 2, pp. 150–160, 2007.

[77] H. Dypvik, "Geochemical compositions and depositional conditions of Upper Jurassic and Lower Cretaceous Yorkshire clays, England," *Geol. Mag.*, vol. 121, no. 5, pp. 489–504, 1984.

[78] H. Dill, "Metallogenesis of early Paleozoic graptolite shales from the Graefenthal Horst (northern Bavaria-Federal Republic of Germany)," *Econ. Geol.*, vol. 81, no. 4, pp. 889–903, 1986.

[79] B. Jones and D. A. C. Manning, "Comparison of geochemical indices used for the interpretation of palaeoredox conditions in ancient mudstones," *Chem. Geol.*, vol. 111, no. 1–4, pp. 111–129, 1994.

[80] T. Toulkeridis, N. Clauer, A. Kröner, T. Reimer, and W. Todt, "Characterization, provenance, and tectonic setting of Fig Tree greywackes from the Archaean Barberton greenstone belt, South Africa," *Sediment. Geol.*, vol. 124, no. 1–4, pp. 113–129, 1999.

[81] T. McCann, "Petrological and geochemical determination of provenance in the southern Welsh Basin," *Geol. Soc. London, Spec. Publ.*, vol. 57, no. 1, pp. 215–230, 1991.

[82] J. B. Murphy, "Tectonic influence on sedimentation along the southern flank of the late Paleozoic Magdalen basin in the Canadian Appalachians: Geochemical and isotopic constraints on the Horton Group in the St. Marys basin, Nova Scotia," *Geol. Soc. Am. Bull.*, vol. 112, no. 7, pp. 997–1011, 2000.